Bull. Mater. Sci., Vol. 32, No. 1, February 2009, pp. 93–98. © Indian Academy of Sciences.

Influence of seeding on crystallization behaviour of $BaNaB_9O_{15}$ glasses

RAHUL VAISH and K B R VARMA*
Materials Research Centre, Indian Institute of Science, Bangalore 560 012, India

MS received 18 August 2008

Abstract. **Transparent $BaNaB_9O_{15}$ (BNBO) glasses were fabricated via the conventional melt-quenching technique. X-ray powder diffraction (XRD) followed by differential scanning calorimetric (DSC) studies confirmed the amorphous and glassy nature of the as-quenched samples, respectively. The effect of seeding on the crystallization of BNBO glasses was studied by non-isothermal DSC method and was modeled using the Johnson–Mehl–Avrami and Ozawa equations. The activation energy for seeded glasses decreased with the increase in fraction of crystallization. The values for the onset of crystallization and Avrami exponent were found to be lower for seeded samples which were associated with the heterogeneous nucleation and epitaxial processes.**

Keywords. **Borates; glasses; nonlinear optic materials; crystallization; DSC.**

1. Introduction

Noncentrosymmetric borate-based compounds have been becoming increasingly important, because of their symmetry dependent properties such as piezoelectricity, pyroelectricity, ferroelectricity and non-linear optical properties. Various borate-based single crystals, including LiB_3O_5 (Wang *et al* 1995), $CsLiB_6O_{10}$ (Nishioka *et al* 2005), $La_2CaB_{10}O_{19}$ (Jing *et al* 2006) have been investigated and reported to be promising from their physical properties view point. These compounds are very attractive particularly for their applications in non-linear photonics. The aforementioned noncentrosymmetric borate single crystals are the most promising among the other noncentrosymmetric compounds for non-linear optical based devices because of their wide optical transmission window, moderate melting points, high laser-induced damage threshold, low cost and good chemical and mechanical stability. Unfortunately growing large single crystals of these materials from their melts is difficult because of their high viscosities. Therefore, we have been exploring alternative ways of obtaining transparent materials. One of the routes that attracted our attention has been the glass–ceramic.

It would be interesting to visualize the physical properties of nano/micrometer sized polar crystallites embedded in a glass matrix as these are known to exhibit exotic properties. The transparent glasses embedded with polar nano/micro crystals could be tailored to exhibit nonlinear optical properties depending on the crystallite size and volume fraction. These are also of technological prominence because of the fact that the microstructure could be engineered precisely for specific applications via controlled heat-treatment of the as-quenched glasses. Controlled crystallization of the glasses has led to the development of glass–ceramic with the desired crystallites size, shape and morphology. A number of techniques have been developed for the fabrication of glass–ceramics with controlled crystallization, keeping specific physical properties in view (Ding *et al* 1994; Honma *et al* 2006; Souza *et al* 2007). In the recent past, several researchers have investigated the influence of seeding on the crystallization of the desired phases in a variety of glass matrices (Selvaraj *et al* 1991; Liu *et al* 1992, 1994; Höland *et al* 1995).

We have been making systematic attempts to fabricate noncentrosymmetric borate based materials in glass–ceramic form for multi-farious applications (Senthil Murugan *et al* 2001, 2002; Syam Prasad *et al* 2003). Recently, BNBO was reported to be belonging to the noncentrosymmetric space group ($R3c$) (Penin *et al* 2001). Since, it is polar and good glass former, we thought it was worth attempting to grow nano/micro crystallites of BNBO in its own transparent glass matrix and visualize their physical properties. For this, it is essential to have *apripori* knowledge about crystallization processes in these glasses. Also, the studies concerning the seeding effect (which would help in achieving the crystallization at lower temperatures) on the crystallization kinetics are in order.

Thermal analyses methods such as differential thermal analysis (DTA) and DSC could frequently be used to study the crystallization processes in amorphous materials. For examining the effect of seeding on the crystallization

*Author for correspondence (kbrvarma@mrc.iisc.ernet.in)

kinetics, non-isothermal methods are employed. The values of crystallization kinetic parameters are calculated and compared with those obtained using Johnson–Mehl–Avrami (JMA) equation in non-isothermal experiments.

2. Experimental

BNBO transparent glasses were fabricated via the conventional melt-quenching technique. For this, $BaCO_3$ (99·95%, Aldrich), Na_2CO_3 (99·9% Merck) and H_3BO_3 (99·9% Aldrich) were mixed in stoichiometric ratio and melted in a platinum crucible at 1373 K for 30 min. Melts were quenched by pouring on a steel plate that was maintained at 423 K and pressed with another plate to obtain 1–2 mm thick transparent glass plates. These glasses were annealed at 673 K (for 10 h) which is well below the glass-transition temperature. The amorphous nature of the samples was confirmed by X-ray powder diffraction (Philips PW1050/37) using CuKα radiation.

Polycrystalline powder comprising 5–10 μm sized crystallites of BNBO that was used for seeding was obtained via the solid-state synthesis route by heating a stoichiometric mixture of reagent grade Na_2CO_3, $BaCO_3$ and H_3BO_3 at appropriate temperatures. XRD studies confirmed the monophonic formation of BNBO. For examining the seeding effect on the crystallization of BNBO bulk glasses, as-quenched polished glass-plates were dipped in acetone containing powdered BNBO for a couple of minutes and then oven dried. The crystallization behaviour of the seeded and unseeded BNBO glass plates was studied using a DSC (Diamond DSC, Perkin-Elmer). For non-isothermal experiments, both seeded and unseeded glasses were heated from 823–973 K at different heating rates (5, 10, 15 and 20 K/min) in nitrogen ambience.

3. Results and discussion

The XRD pattern obtained for the as-quenched sample that is shown in figure 1 confirms its amorphous state. In figure 2(a–c), we show the typical DSC traces recorded for seeded, unseeded BNBO glass plate along with that of the powdered samples at a heating rate of 10 K/min. The glass transition temperature (T_g) and the onset of crystallization temperature (T_{cr}) are identified as the temperatures corresponding to the intersections of the two linear portions of the transition (glass transition and crystallization) elbows of the DSC traces. At the heating rate of 10 K/min, the onset of crystallization temperatures obtained for seeded, unseeded plate and powdered samples are 894 K, 913 K and 884 K, respectively. It is noticed that the powdered BNBO glass sample exhibits a relatively sharp exothermic peak (figure 2(c)) at a lower temperature than those of the other two samples. This is due to the fact that the glass powder (higher surface area) is more sensitive to the absorption of heat energy in the non-isothermal experiments. This indicates that the nucleation and growth of the powdered BNBO glass sample could be initiated at lower temperatures. The glass transition temperature, T_g, remains to be almost the same (805 K) for all the samples under study. Asymmetrical crystallization peak is observed in the case of seeded glass plate which implies that the crystallization process is complex. The DSC traces that are obtained for unseeded and seeded BNBO glass plates at different heating rates (5, 10, 15 and 20 K/min) are shown in figures 3(a) and (b), respectively. In both the cases there is an upward shift in the crystallization peaks though it is broad for a seeded plate.

The fraction of crystallization (x) was determined using the partial area technique. The fraction, x, crystallized at any temperature, T, is given by $x = (A_T/A)$ under non-

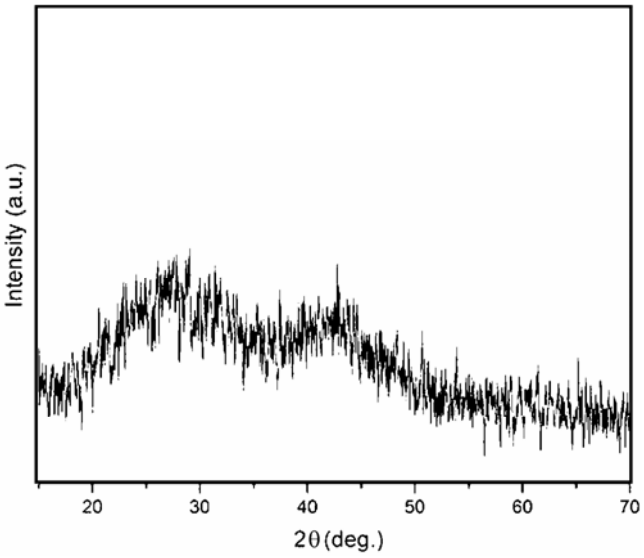

Figure 1. XRD pattern for the as-quenched pulverized $BaNaB_9O_{15}$ glass.

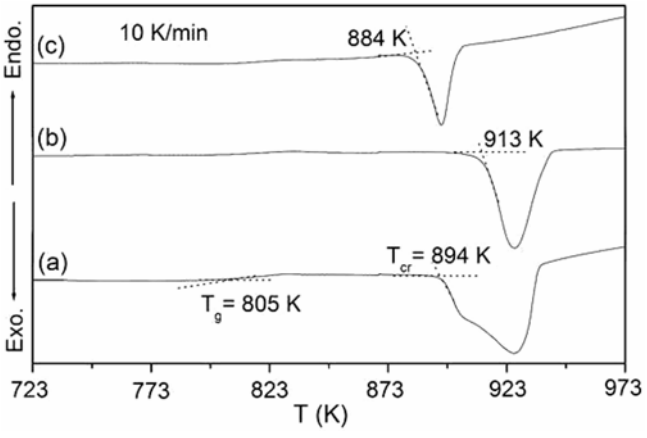

Figure 2. DSC traces for (a) seeded $BaNaB_9O_{15}$ glass plate, (b) unseeded $BaNaB_9O_{15}$ glass plate and (c) powder.

isothermal condition where A_T is the area under the exotherm (crystallization peak) from T_i (from where crystallization begins) to temperature T as shown in figure 4 and A is the total area of the crystallization peak. Using the partial area technique, the fraction of crystallization (x) was calculated at different temperatures and heating rates. Fraction of crystallization vs temperature at different heating rates for seeded BNBO glasses are illustrated in figure 5. Similar sigmoid trends were found for unseeded samples which are not depicted here.

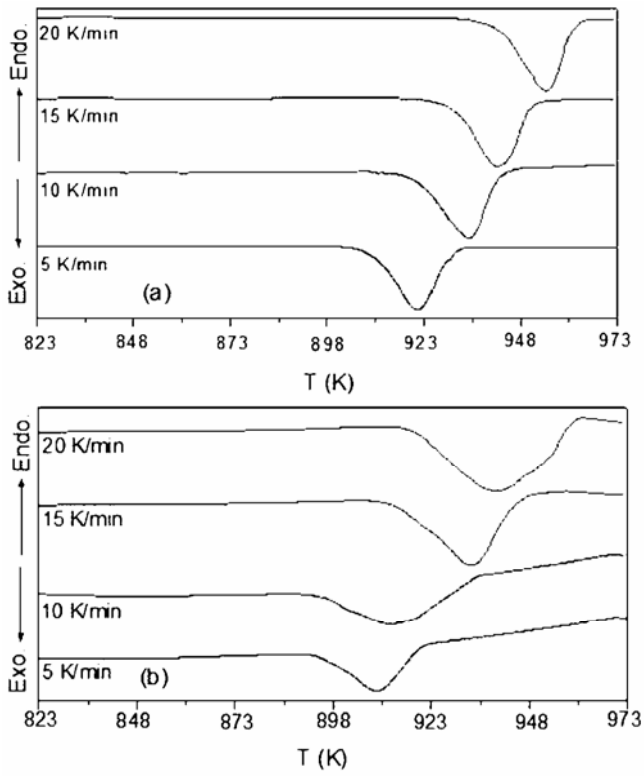

Figure 3. DSC traces for the (a) as-quenched unseeded and (b) seeded $BaNaB_9O_{15}$ glass plates at different heating rates.

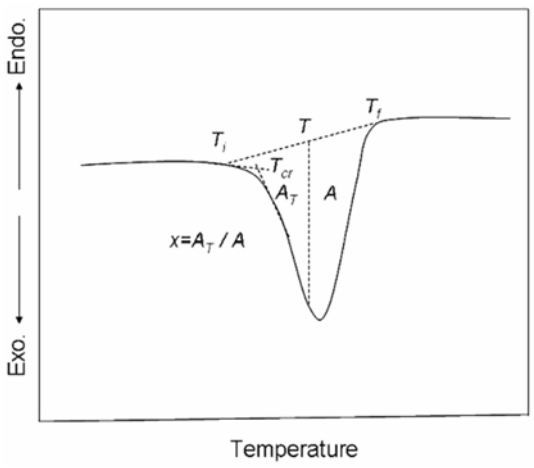

Figure 4. Typical exothermic peak in non-isothermal experiment.

3.1 *Crystallization kinetics*

Crystallization behaviour of the seeded and unseeded BNBO glass was studied by non-isothermal DSC methods. In the non-isothermal studies, DSC measurements were made on the glass plates at various heating rates. Heating rate dependence of the onset temperature of crystallization and crystallization peak temperature was evaluated and analysed for comparing crystallization behaviour of seeded and unseeded glasses using different non-isothermal models.

The Johnson–Mehl–Avrami (JMA) equation (Avrami 1939, 1940, 1941) concerning the kinetics of phase transformation involving nucleation and growth under isothermal conditions is generally used to analyse the crystallization process. It is expressed as

$$x = 1 - \exp[-\{k(t - t_i)\}^n], \tag{1}$$

where k is the rate constant, t the transformation time, t_i the incubation time, n the Avrami exponent which reflects the characteristics of nucleation and growth process and x the crystalline volume fraction. The constant, k, is related to the effective activation energy (E), describing the overall crystallization process and its Arrhenius temperature dependence is given by

$$k = k_0 \exp\left(\frac{-E}{RT}\right), \tag{2}$$

where k_0 is the frequency factor, R the universal gas constant, T the absolute temperature.

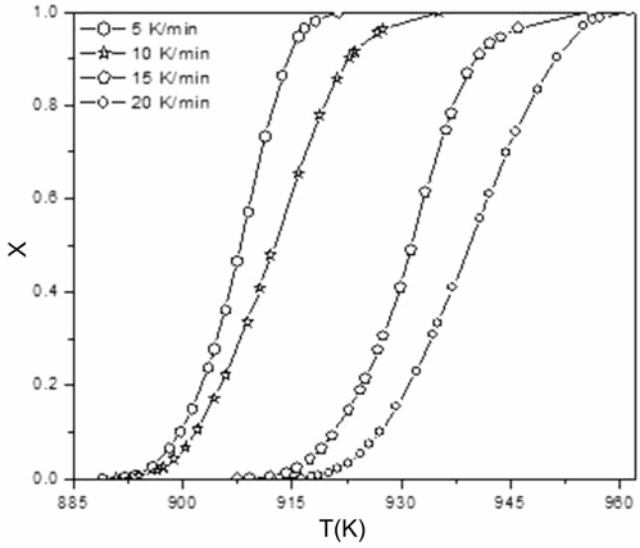

Figure 5. Fraction of crystallization vs temperature curves at various heating rates for seeded BNBO glass plates.

Various theoretical methods have been suggested to understand the nucleation and growth process based on JMA equation using the non-isothermal DSC or DTA data (Yinnon and Uhlmann 1983). All the methods assume a constant heating rate, α, in the DTA or DSC experiments, wherein

$$\alpha = \frac{T - T_i}{t}, \tag{3}$$

where T_i is the initial temperature and T the temperature after time, t. For non-isothermal experiments, (1) when combined with (2) and (3), one arrives at

$$x = 1 - \exp[-(k_0 \exp(-E/RT))^n \times ((T - T_i)/\alpha)^n]. \tag{4}$$

For the applicability of JMA model to the non-isothermal crystallization process, several conditions should be satisfied (Málek 1995). The validity of JMA model in non-isothermal experiments is confirmed by obtaining a linear plot between $\ln[-\ln(1-x)]$ and $(1/T)$ (Málek 1995). The plots of $\ln[-\ln(1-x)]$ vs $1/T$ for unseeded and seeded BNBO glass-plates at different heating rates are depicted in figures 6(a) and (b), respectively. For unseeded glasses, the plots are linear over most temperature ranges as shown in figure 6(a). Some deviations from linearity at high temperatures or in the regions of large crystallized fractions are attributed to the saturation of nucleation sites in the final stage of crystallization (Afify *et al* 1991). Whereas, for the seeded samples (figure 6(b)), the plots are non-linear in the complete crystallization range for all the heating rates under study. In such cases, the crystallization process cannot be modeled using the single JMA expression.

3.1a *Activation energy*: Generally, the value of activation energy associated with crystallization is material and thermal history dependent. It is observed in various glass systems that it also depends on the fraction of crystallization (Joraid 2007; Joraid *et al* 2008). A local activation energy, $E_c(x)$, is the activation energy at a stage when the crystallized volume fraction is x, which is applied to describe the crystallization behaviour that reflects the change in nucleation and growth behaviour in the crystallization process. The local activation energies for the crystallization of seeded and unseeded BNBO glass plates were determined using a method introduced by Ozawa (1986) according to which

$$\left[\frac{\partial \ln \alpha}{\partial (1/T)}\right]_x = -\frac{E_C(x)}{R}, \tag{5}$$

where T and α are the temperature and heating rate corresponding to fixed values of x. The values of $E_c(x)$ were obtained from the slopes of $\ln\alpha$ vs $1000/T$ plots at different fractions of crystallization for both the seeded and unseeded samples. The plots of $E_c(x)$ vs x for both the samples are shown in figure 7. It is observed that $E_c(x)$ is invariant during the crystallization process for unseeded glass plate. The invariant activation energy of crystallization shows validity of JMA model for unseeded BNBO glasses. The average value for activation energy is 338 kJ/mol whereas for the seeded BNBO glasses, the change of $E_c(x)$ with increasing x is an indication of a variable crystallization process. It is seen that at the initial crystallization stage, the activation energy for crystallization of BNBO is 335 kJ/mol, which is very close to that obtained for unseeded sample. As the crystallization proceeds, the activation energy decreases drastically and remains almost constant with the crystallized volume fraction exceeding 0·4. It indicates that the crystallization rate is higher during initial stage of crystallization. When the crystallized volume fraction lies in the range of 0·4–0·9, the average activation energy of the seeded sample is about 287 kJ/mol during the non-isothermal transformation process.

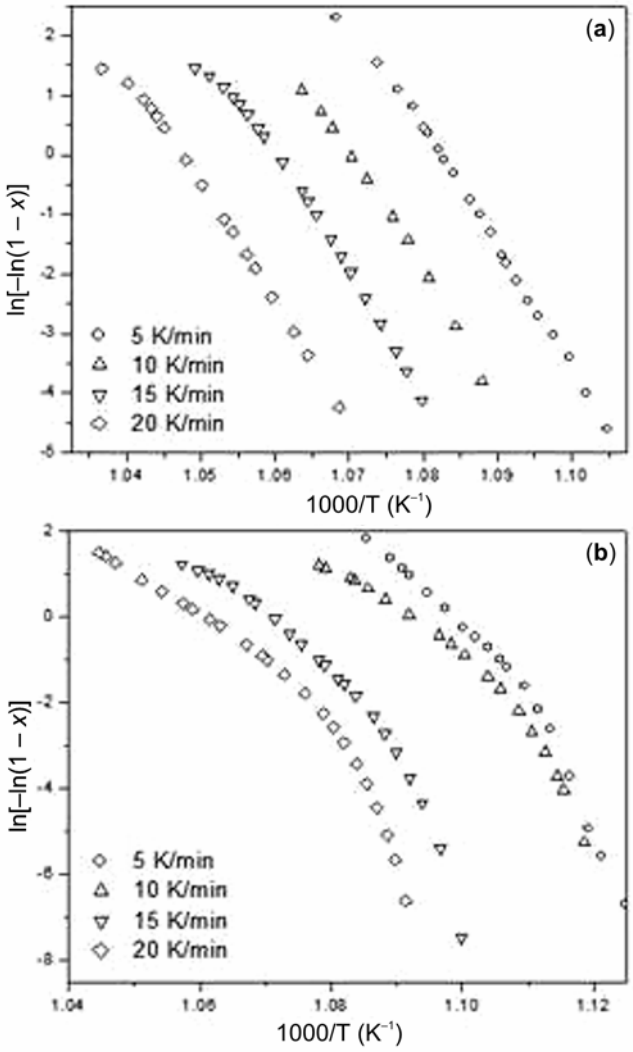

Figure 6. $\ln[-\ln(1-x)]$ vs $1000/T$ plots for (**a**) unseeded and (**b**) seeded BNBO glass plates at various heating rates.

The activation energy for crystallization process (E_c) consists of two components: the activation energy for the nucleation (E_n) and for the growth (E_g) (Yinnon and Uhlmann 1983):

$$E_c = aE_n + bE_g, \tag{6}$$

where a and b are positive constants related to the Avrami exponent and $a + b = 1$.

For seeded glasses, the early stage of crystallization is dominated by the nucleation and crystallization processes and as the temperature increases only the growth process is expected to be active on the preexisting nuclei. Whereas, for unseeded samples, the constant value of activation energy during the crystallization process reflects the steady nucleation and growth processes.

3.1b *Avrami exponent*: Using the values of activation energy, the Avrami exponents for both the samples (unseeded and seeded) were calculated from (4). For fractions of crystallization, x_1 and x_2, at different temperatures, T_1 and T_2, for a non-isothermal run at the heating rate, α, one obtains

$$x_1 = 1 - \exp[-(k_0 \exp(-E_1/RT_1))^n \times ((T_1 - T_i)/\alpha)^n], \tag{7}$$

$$x_2 = 1 - \exp[-(k_0 \exp(-E_2/RT_2))^n \times (T_2 - T_i/\alpha)^n], \tag{8}$$

where E_1 and E_2 are the activation energies at different fractions of crystallization, x_1 and x_2, respectively.

After rearranging and taking logarithmic forms of (7) and (8), one would obtain

$$\frac{\ln(1-x_1)}{\ln(1-x_2)} = \left[\frac{\exp(-E_1/RT_1)}{\exp(-E_2/RT_2)} \times \frac{(T_1 - T_i)}{(T_2 - T_i)}\right]^n. \tag{9}$$

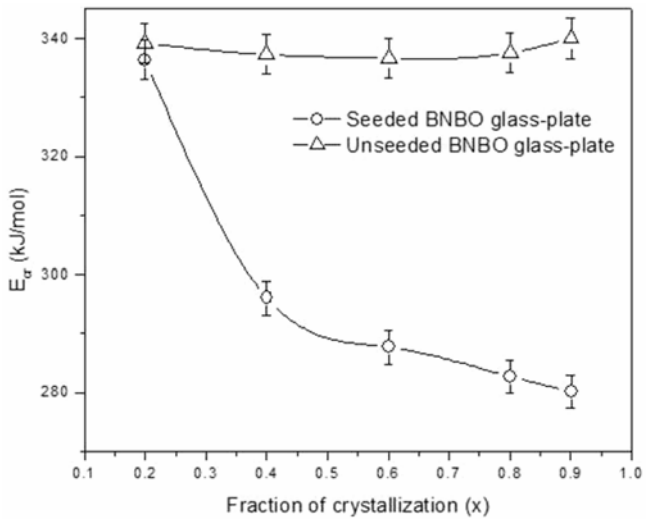

Figure 7. Variation of activation energy with the fraction of crystallization for both the seeded and unseeded glasses.

Taking the logarithm of (9), one arrives at

$$\ln\left[\frac{\ln(1-x_1)}{\ln(1-x_2)}\right] = n\left[\frac{1}{R}\left(\frac{E_2}{T_2} - \frac{E_1}{T_1}\right) + \ln\frac{(T_1 - T_i)}{(T_2 - T_i)}\right]. \tag{10}$$

For unseeded BNBO samples, $E_1 = E_2 = E$ (let), one arrives at

$$\ln\left[\frac{\ln(1-x_1)}{\ln(1-x_2)}\right] = n\left[\frac{E}{R}\left(\frac{1}{T_2} - \frac{1}{T_1}\right) + \ln\frac{(T_1 - T_i)}{(T_2 - T_i)}\right]. \tag{11}$$

The Avrami exponent (n) could be determined using the above equation for unseeded samples. For the unseeded glasses the average value obtained for n is $2{\cdot}5 \pm 0{\cdot}2$ suggesting one and two dimensional bulk crystallization processes to be active. To demonstrate the effect of seeding, the values of n were estimated for the seeded samples using (10) at different crystallization stages. The average value of n is found to be $1{\cdot}5 \pm 0{\cdot}2$, indicating the predominance of surface crystallization process.

4. Conclusions

The effects of seeding on the crystallization kinetics of BNBO glasses have been investigated. The DSC non-isothermal experiments that were carried out on seeded $BaNaB_9O_{15}$ glass plates confirmed the dominance of surface crystallization phenomenon which may be exploited in the fabrication of optical waveguides. The crystallization temperature was found to be lowered for seeded samples due to catalytic effect. The crystallization activation energy for unseeded sample was 338 kJ/mol, whereas it was found to be varying with the fraction of crystallization for seeded glasses. However, the Avrami exponent does not vary with the fraction of crystallization for both unseeded and seeded samples and its average values were $2{\cdot}5 \pm 0{\cdot}2$ and $1{\cdot}5 \pm 0{\cdot}2$, respectively. Decrease in Avrami exponent shows an enhancement in surface crystallization.

References

Afify N, Abdel-Rahim M A, Abd El-Halim A S and Hafiz M M 1991 *J. Non-Cryst. Solids* **128** 269

Avrami M 1939 *J. Chem. Phys.* **7** 1103

Avrami M 1940 *J. Chem. Phys.* **8** 212

Avrami M 1941 *J. Chem. Phys.* **9** 177

Ding Y, Osaka A and Miura Y 1994 *J. Am. Ceram. Soc.* **77** 749

Höland W, Frank M and Rheinberger V 1995 *J. Non-Cryst. Solids* **180** 292

Honma T, Benino Y, Fujiwara T and Komatsu T 2006 *Appl. Phys. Lett.* **88** 231105

Jing F, Wu Y and Fu P 2006 *J. Crystal Growth* **292** 454

Joraid A A 2007 *Thermochim Acta* **456** 1

Joraid A A, Alamri S N and Abu-Sehly A A 2008 *J. Non-Cryst. Solids* **354** 3380

Liu C, Komarneni S and Roy R 1992 *J. Am. Ceram. Soc.* **75** 2665
Liu C, Komarneni S and Roy R 1994 *J. Am. Ceram. Soc.* **77** 3105
Málek J 1995 *Thermochim. Acta* **267** 61
Nishioka M, Kanoh A, Yoshimura M, Mori Y and Sasaki T 2005 *J. Crystal Growth* **279** 76
Ozawa T 1986 *J. Therm. Anal.* **31** 547
Penin N, Seguin L, Touboul M and Nowogrocki G 2001 *Int. J. Inorg. Mater.* **3** 1015
Selvaraj U, Komarneni S and Roy R 1991 *J. Mater. Sci.* **26** 3689
Senthil Murugan G, Varma K B R, Takahashi Y and Komatsu T 2001 *Appl. Phys. Lett.* **78** 4019
Senthil Murugan G and Varma K B R 2002 *J. Mater. Chem.* **12** 1426
Souza J E D, Peko J C M and Hernandes A C 2007 *Appl. Phys. Lett.* **91** 064105
Syam Prasad N, Varma K B R, Takahashi Y, Benino Y, Fujiwara T and Komatsu T 2003 *J. Solid State Chem.* **173** 209
Yinnon H and Uhlmann D R 1983 *J. Non-Cryst. Solids* **54** 253
Wang Y, Jiang Y J, Liu Y L, Cai F Y and Zeng L Z 1995 *Appl. Phys. Lett.* **67** 2462